

Article

Not peer-reviewed version

# Physicochemical Properties and In Vitro Dissolution of Edible Film Based on Starch-Chitosan Used as a Potential Oral Drug Carrier: Model Using Acetaminophen

[Carolina Caicedo](#)\*, [Natalia Ramírez](#), Leidy Portilla, Laura Saldaña, [Abril Foseca-García](#)

Posted Date: 19 February 2025

doi: 10.20944/preprints202502.1487.v1

Keywords: Orally disintegrating films; disintegration time; mechanical properties; biopolymers; thermal analysis



Preprints.org is a free multidisciplinary platform providing preprint service that is dedicated to making early versions of research outputs permanently available and citable. Preprints posted at Preprints.org appear in Web of Science, Crossref, Google Scholar, Scilit, Europe PMC.

Copyright: This open access article is published under a Creative Commons CC BY 4.0 license, which permit the free download, distribution, and reuse, provided that the author and preprint are cited in any reuse.

*Article*

# Physicochemical Properties and In Vitro Dissolution of Edible Film Based on Starch-Chitosan Used as a Potential Oral Drug Carrier: Model Using Acetaminophen

Carolina Caicedo <sup>1,\*</sup>, Natalia Ramírez Giraldo <sup>2</sup>, Leidy Portilla <sup>3</sup>, Laura Saldaña <sup>3</sup>  
and Abril Fonseca García <sup>4,5,\*</sup>

<sup>1</sup> Grupo de Investigación Energías, Facultad de Ingeniería, Unidad Central del Valle del Cauca (UCEVA), Carrera 17a 48-144, Tuluá 763022, Colombia

<sup>2</sup> Semillero de Investigación en Ciencia e Ingeniería de Materiales (CIMAT), Facultad de Ingeniería, Unidad Central del Valle del Cauca (UCEVA), Carrera 17a 48-144, Tuluá 763022, Colombia

<sup>3</sup> Semillero de Investigación en Química Aplicada (SEQUIA), Facultad de Ciencias Básicas, Universidad Santiago de Cali, Pampalinda, Santiago de Cali 760035, Colombia

<sup>4</sup> Centro de Investigación en Química Aplicada (CIQA), Blvd. Enrique Reyna Hermosillo 140, Saltillo, Coahuila 25294, México

<sup>5</sup> Investigadoras e investigadores por México de SECIHTI, Av. Insurgentes Sur 1582, Col. Crédito Constructor, Delegación Benito Juárez. 03940, Ciudad de México

\* Correspondence: ccaicedoc@uceva.edu.co

**Abstract:** This work aimed to evaluate the effect of incorporating a type model active pharmaceutical ingredient in an orally disintegrating film (ODF) based on starch and chitosan on the physicochemical and thermodynamic surface properties. The ODFs were formed using the solvent casting method, with a thickness of 0.04 mm. Chemical analysis performed by vibrational spectroscopy showed strong intermolecular interactions between the components of the polymeric matrix. XRD structural analysis confirmed these interactions from the decrease in crystallinity in the biopolymeric compounds; the active pharmaceutical ingredient did not present changes in the ordering. The inclusion of the drug maintained the hydrophilicity with contact angle values around 62°. However, the water absorption values had increased for the TPS-CH-M-A film by ~90%. The adequate particle dispersion was shown in the SEM of acetaminophen which facilitated the opening of the polymer chains, which increased the soluble solids content in contact with water. Also, the mechanical properties were not affected by the incorporation of acetaminophen particles, the tensile strength values of the polymeric blend were around 24 MPa and the elongation at break was around 4.0%, in the ODF the toughness increased by 8%. These factors allowed disintegration times of 48 s, in vitro dissolution times of 10 min to release ~73% of acetaminophen, and 15 min to release all the active ingredients. Therefore, the chitosan starch-based ODF containing acetaminophen represents a promising system for use in the delivery of pharmaceutical active ingredients.

**Keywords:** orally disintegrating films; disintegration time; mechanical properties; biopolymers; thermal analysis

## 1. Introduction

The oral administration of drugs through conventional dosage forms such as capsules, dragees, and tablets, among others, presents limitations when administered to geriatric, pediatric, dysphagic, psychiatric, and even animal patients.[1] One of the main causes corresponds to neuromuscular changes, however, but it can also occur in patients with neurocognitive disorders.[2] Studies that

have evaluated dysphagia document a prevalence in people over 65 years of age, around 30% of elderly people admitted to a hospital, being considered a new geriatric syndrome. On the other hand, a prevalence of 50% is estimated for elderly residents of nursing homes, and more than 40% corresponds to patients who have suffered strokes.[2] Given these needs, orodispersible dosage forms have been proposed, which have been shown to overcome these limitations. An alternative method of administration is orally disintegrating films (ODFs), based on polymers, they are thin (thicknesses  $>10\text{ }\mu\text{m}$  y  $<750\text{ }\mu\text{m}$ )[3], flexible, easy to administer, and stable in preparation, packaging, and transportation.[1-4] ODFs are generally composed of water-soluble polymers, plasticizers, and an active component. These are hydrated adhere to the oral mucosa and release the drug for transmucosal or local therapy. Buccal transmucosal administration is a noninvasive route for systemic administration that provides advantages over oral administration. Because it offers a faster action due to the vascularization of the mucosa. This improves bioavailability and prevents enzymatic degradation of the gastrointestinal tract and first-pass metabolism.[5] Additionally, easy access to the oral cavity and buccal mucosa improves the application and removal of a drug delivery system to make it simple for the patient and caregiver. However, saliva constantly rinses the oral mucosa, and movements of the tongue and jaw can limit its usefulness. On the other hand, it is known that the drug permeability of the oral mucosa is lower compared to the small intestine, although the low permeability can be compensated with a longer retention time.[6] There are two types of oral films, orodispersible ones that aim for rapid dissolution, bioadhesiveness that allows high solubility, and absorption that leads to the bioavailability of the drug.[7] And, the mucoadhesive films that are Intended for application on the oral mucosa, remain long enough and adequate to release the active components in a controlled manner.

Therefore, the polymer matrix that allows the transport of the active ingredient requires integrating characteristics of several compounds in which the application is enhanced. The intrinsic properties of the polymers constitute a fundamental part of the synergy of the formulations. Biopolymers based on polysaccharides play a fundamental role due to the ability to form films in the presence of plasticizers and the organoleptic properties that they provide to the matrix-drug system. Among the biopolymers that allow the manufacture of edible films from solutions, starch, and chitosan have been widely studied, considering optimal ratios of 1.5:1, respectively, in which excellent mechanical properties have been obtained. Always seeking to enhance the flexibility of thermoplastic starch (TPS) with the rigidity of chitosan.[8] It has been shown through studies that chitosan-based ODFs contain high mucoadhesiveness since having a positive charge on the amino group generates a strong electrostatic interaction with the negative charge of salic acid residues present in the mucosa.[9] Disintegration times have also been demonstrated below 36 s and when mixed with various plasticizers such as glycerol or sorbitol, chitosan films have high tensile strength and flexibility. The versatility of chitosan lies in its biocompatibility, non-toxicity to humans, and biodegradability. In addition, it has antioxidant and antimicrobial activity and the ability to form homogeneous films.[10] On the other hand, starch is a non-ionic polysaccharide, which is characterized by having less mucoadhesiveness; however, its relationship with the mucosa is achieved by the interpenetration of the polymer chains. Starch has been used in recent years for the development of thin films for drug delivery.[11] Depending on the botanical source from which it is obtained, it has specific compositions and microstructural rearrangements that relate crystallinity that lead to different physicochemical and biological properties. Cassava starch is characterized as a good option for the development of ODF since it has been shown to have low disintegration times with an order of 10 s and high tensile strength with an order of 30 MPa.[12,13] Multiple studies show the synergy between starch and chitosan in films that present excellent antimicrobial properties, which allow various applications including the agricultural and food sector as coatings for fruits to prolong shelf life.[14] On the other hand, the development of microparticles from unconventional manufacturing techniques such as spray drying of starch-chitosan mixtures in the presence of surfactants in which a bowl-shaped morphology is guaranteed, which allows a potential for another range of applications related to microencapsulation.[15] Another carbohydrate with potential

participation as an ingredient in the biofilm matrix is maltodextrin, an oligomer derived from starch, formed by ~10 glucose units. It is a good ODF forming agent with good mechanical properties (high ductility)[16] and short disintegration times due to its hydrophilic nature.[17] Amylose has been used for its encapsulation capacity, it is colorless, and it provides thermal and oxidation protection.[18,19] This exhibits high flexibility, which makes maltodextrin a promising polymer for application in ODF as a formulating agent alone or mixed with other macromolecules. Among the most used techniques for the manufacture of ODF are solvent casting, hot fusion extrusion, and other non-conventional techniques such as additive manufacturing technologies (inkjet printing, semisolid extrusion 3D printing, and fused deposition modeling 3D printing). The solvent-casting technique consists of dissolving the active compound, film-forming polymers, and additives in a suitable solvent to form a viscous solution or suspension, which is then uniformly poured into a pre-designed mold for the subsequent drying process. The films obtained are characterized considering the uniformity of the content, the thickness of the film, and the morphology, among others.[5]

In general, oral disintegration films allow the incorporation of active pharmaceutical ingredients (API) that can be released in a controlled manner, interest in the manufacture of ODF by pharmaceutical companies has not been limited to mass production, nor personalized medicine. Acetaminophen (A) is one of the most consumed drugs worldwide, due to its therapeutic safety, effectiveness, and accessibility.[20] Acetaminophen is an n-acetyl-p-aminophenol derived from phenacetin, its molecular weight is low (151 Dalton) and it has weak acid behavior. It is marketed in the form of capsules or tablets (film-coated tablets, effervescent tablets) suitable for crushing (not liquid forms of the drug), each containing 500, 650, or up to 1000 mg.[21] There are also presentations in liquid form such as drops and syrup. Additionally, a rapid and effective analgesic and antipyretic action has been proven in infants, children, adolescents, and adults similar to that of acetylsalicylic acid. Although it does not have the anti-inflammatory capacity of salicylates, it has been used satisfactorily in patients who have an allergy or intolerance to aspirin.[22] Therefore, the effect of incorporating a type model active pharmaceutical ingredient in an oral disintegrating film (ODF) based on starch and chitosan on the physicochemical and thermodynamic surface properties was evaluated.

## 2. Materials and Methods

### 2.1. Materials

The following biopolymers were used: Native Cassava starch variety SM 707-17 (*Manihot esculenta* Crantz) from the "La Agustina" grating factory, located in Mondomo, Cauca, Colombia. The starch had a density of 1.58 g/mL; maltodextrin (Agenquímicos Ltd., Cali, Colombia), chitosan was supplied by the supplier Sigma Aldrich, low molecular weight, degree of deacetylation >75%, and Glycerol with a density of 1.26 g/mL (purity: 99.68%). Buffer solution (di-sodium hydrogen phosphate/potassium dihydrogen phosphate), traceable to SRM from NIST and PTB pH 7.0 (20 °C) Certipur® Marca Sigma-Aldrich. Glacial acetic acid 100% anhydrous was obtained from the supplier Merck. Finally, certified reference material grade acetaminophen, a secondary pharmaceutical standard Sigma-Aldrich brand, was used.

### 2.2. Preparation of Oral Disintegrating Films

#### 2.2.1. Preparation of Film-Forming Solutions

An aqueous solution (TPS) of starch and glycerin was prepared with a concentration of 5% (w/v) and 1.25% (w/v), respectively. This solution was homogenized by magnetic stirring at 700 rpm, and in turn, was subjected to heating until reaching a temperature of 70 °C for 10 min. Subsequently, the stirring was increased to 1200 rpm as the gelatinization of the polymer solution was observed. In parallel, a 2% (w/v) solution of chitosan in 1% glacial acetic acid was prepared. This solution was homogenized using magnetic stirring at 1000 rpm at room temperature for 30 min, during which time



complete dissolution of the chitosan was observed. A third 5% (w/v) aqueous maltodextrin solution was prepared. This solution was homogenized by magnetic stirring at 300 rpm at room temperature until the maltodextrin was completely dissolved.

### 2.2.2. Preparation of Biopolymeric Films

The films were made according to the solvent-casting method. From the previously prepared solutions, the filmogenic solution is composed by a ratio of 60:20:20 of polymeric solutions of TPS: chitosan: maltodextrin (TPS-CH-M) were taken. The resulting film-forming solution was stirred for 10 min at 500 rpm and was subsequently subjected to ultrasound (Elmasonic Easy 120 H for 10 min, 27 kHz, 200 W at 25 °C, it was subjected to a vacuum to eliminate the air bubbles present.

The polymer solution was poured into a cylindrical mould ensuring a height of 0.17 mm. This was previously tested to obtain a film with a thickness of less than 0.05 mm, in all cases according to recommendations found in the literature [1]. It was then dried in a forced ventilation oven (Binder, series 14291) for 3 h at 65 °C. The films were demolded and conditioned for 48 h at 25 °C and 50% RH before evaluating their physical and chemical properties. Five random thickness measurements of five films were made with a  $150 \pm 0.1$  mm caliper (Fischer Darex) and resulted in an average thickness value of  $0.038 \pm 0.004$  mm.

### 2.2.3. Preparation of Biopolymeric Films Containing a Pharmaceutical Ingredient

The same process and concentrations of the polymers used in the preparation of the matrix previously described were established, and acetaminophen (A) was incorporated. It was carried out by trial and error taking into consideration the homogeneity and film-forming capacity using a ratio of volume of filmogenic solution: mass of drug: 90:10, 95:5, 97:3, 91:1, 99.5:0.5, 99.75:0.25 (see Figure S1), Supplementary information). According to the above, the maximum drug loading selected was 99.5:0.5. The preparation consisted of adding the type model such as acetaminophen to the first solution (TPS solution) before heating, the mass amount added was such that it ensured obtaining 0.5% API in the final filmogenic solution. The addition continued into the molds for drying and forming the film, reaching a height of 0.17 mm in the cylinder. The films were conditioned for 48 h at 25 °C and 50% RH before evaluating their physical and chemical properties. Five random measurements were made of 5 films made with API where an average value equal to  $0.044 \text{ mm} \pm 0.005 \text{ mm}$  was obtained. Likewise, the surface pH was measured (with a multiparameter pH meter with 2 channels, Hanna, HI5522). The readings were taken after keeping the ODF in contact with distilled water at 37 °C for 30 s. Three (3) repetitions were carried out taking 10 different films. The average pH value for films with API was  $6.651 \pm 0.004$ , and the average pH value for films without acetaminophen was  $6.758 \pm 0.011$ , these did not show significant differences.

## 2.3. Characterization of Biopolymeric Films

### 2.3.1. Pharmaceutical Active Ingredient (API) Quantification

The determination was carried out in a UV-Vis spectrophotometer (Merck, spectroquant prove 600) at 243 nm. The curve was prepared in 0.1 M HCl solution taking 5 points of defined concentrations (0.02, 0.2, 0.4, 0.6, and 0.8%). [23] These are from a stock solution prepared with acetaminophen (A) at 99% purity. The films with API were dissolved in an aqueous solution buffered at pH 6.8 at 37 °C with constant stirring at 50 rpm for 30 min. [24] After time, the solution was filtered by gravity through 90 mm qualitative filter paper (Boeco, Germany), and then through a nylon syringe filter with a pore size of  $0.45 \mu\text{m}$  (Fisher Scientific). Readings were performed at 243 nm using a film without API as a control.

### 2.3.2. Fourier Transform Infrared Spectroscopy (FTIR)

The analysis was carried out under Fourier transform infrared spectroscopy using KBr pellets. This analysis allowed us to know the different types of vibrations experienced by the bonds in the organic compound and the influence of its molecular environment. A Shimadzu spectrophotometer, model IR Affinity-1, was used. The spectra were recorded between 400  $\text{cm}^{-1}$  and 4000  $\text{cm}^{-1}$  at a resolution of 4  $\text{cm}^{-1}$  at 45 scans.

### 2.3.3. X-Ray Diffraction Analysis

The atomic arrangement of films was observed by X-ray diffraction (XRD) using Malvern-Panalytical equipment (Empyrean model, Worcestershire, United Kingdom). The measurements were done by Bragg-Brentano configuration of powder diffraction and platform (goniometer: Omega/2 theta, and platform configuration: Reflection Transmission Spinner with 4 s rotation). The step was 0.02° and the time per step was 52 s. The measurement was made under the condition, that Cu X-ray radiation was generated at 45 kV, 40 mA, and Cu  $K\alpha = 1.541 \text{ \AA}$ .

### 2.3.4. Simultaneous Thermal Analysis: Thermogravimetric Analysis (TGA), Differential Scanning Calorimetry (DSC).

The thermal properties were studied using a TGA/DSC 2 STAR System thermogravimetric analyzer from Mettler Toledo (Schwerzenbach, Switzerland). The thermal degradation behavior and first and second-order temperature transitions were analyzed. The heating rate was 20 °C/min, heated from its starting temperature of 25 °C to a final temperature of 600 °C. The system was fed by nitrogen that flowed at a rate of 50 mL/min over  $10 \pm 0.5 \text{ mg}$  of material.

### 2.3.5. Mechanical Tests

The mechanical behavior was analyzed by calculating the tensile strength (TS) and the percentage of elongation at break (%E). The tests were carried out based on the ASTM standard (D882-12)[25], using a universal testing machine from the Hung TA Instrument Go brand. The test speed was 20 mm/min using rectangular specimens 2.5 cm wide and 12.0 cm long. Values were taken guaranteeing the reading of 5 films fractured in the center, this for films with and without drug content.

### 2.3.6. Scanning Electron Microscopy

The morphology analysis of the films was performed using a JCM 50000 instrument (JEOL, Tokyo, Japan) in the secondary electron mode at 10 kV. Film preparation was performed by fracturing the samples after freezing them in liquid N<sub>2</sub>. For this measurement, the samples were placed on carbon tape and gold-coated using a direct current sputter technique. Magnifications of 1500X, 1000X, 500X, and 100X of the fracture surface were taken.

### 2.3.7. Measurement of Sessile Drop

Contact angle measurements were performed using a goniometer (Ramé-Hart Instrument Co., Ltd., model 250, Succasunna, New Jersey, USA), with the addition of 20  $\mu\text{L}$  of water at 25 °C on the polymer after 30 s. The image was recorded and the contact angle was measured using the free software ImageJ version 5.0.3. The results were obtained by averaging five measurements for each sample.

### 2.3.8. Absorption (Swelling) Test

The films were cut into a size of 1  $\text{cm}^2$  and the weight was recorded as the initial weight ( $W_0$ ) of the film. Then, the film samples were immersed in water at 23 °C and the weight of the samples was recorded at predetermined time points (5, 10, 15, 30, 45, and 60 min). Excess water on the surface was

carefully removed from the swollen films with filter paper to report the final weight ( $W_f$ ). [26,27] The percentage gain from the sample for three replicates was calculated according to the following equation:

$$\text{Absorption weight gain (\%)} = (W_f - W_0) / W_0 * 100 \quad (1)$$

### 2.3.9. Disintegration Time

#### In Vitro Oral Disintegrating Time

The in vitro disintegration time of the films was analyzed, using a chronometer that allowed us to know the initial time ( $T_0$ ) and final time ( $T_f$ ) that the test lasted. Samples were cut 2 cm x 3 cm wide by length, respectively. These were placed in petri dishes and kept completely flat, and 200  $\mu$ L of distilled water at 37 °C was added to the surface of the film. The  $T_0$  was indicated at the exact moment in which the water content was added, and the final time ( $T_f$ ) when the first perforation showed. Thus, the disintegration time was calculated as the difference of  $T_f$  and  $T_0$ . [28]

#### In Vitro Dissolution Time

The determination was carried out in a UV-VIS spectrophotometer (Merck, spectroquant prove 600) at 243 nm. The test consisted of dissolving 1.0 g of the film with acetaminophen in 25 mL of aqueous solution buffered at pH 6.8, maintaining a temperature of 37 °C with constant stirring at 50 rpm. [29] After 180 s, the solution was filtered by gravity through 90 mm qualitative filter paper (Boeco, Germany) and subsequently through a nylon syringe filter with a 0.45  $\mu$ m pore (Fisher Scientific). Finally, the concentration of the film was measured for specific periods: 5, 8, 10, 15, and 30 min.

#### Sugars Determination (°Brix)

Total soluble solids (TSS) concentration in Brix (°) of the films with and without acetaminophen was measured under the official protocol (AOAC, 2012) [30] using a digital refractometer, ATAGO brand, reference: Pocket Refractometer PAL-3. Range 0-93%. The apparatus was calibrated with deionized water (refraction index = 1.3330 and °Brix at 37 °C and the measurements of the samples were taken (°Brix). ~0.2 g of sample was weighed and immersed in 5 mL of distilled water at 37 °C, maintaining the temperature throughout the test. 0.5 mL of the solution (distilled water in contact with the film) was taken at 5, 8, 10, 15, and 30 min to measure. The following conditions were available for the analysis without stirring and with magnetic stirring at 50 rpm, at 37 °C, for both cases.

#### Statistical Analysis

Means and standard deviations are presented, and analysis of variance (ANOVA) was used to compare mean differences in film characteristics. In addition, the comparison of means was performed using Tukey's test at a significance level of 0.05. All statistical analyses were performed using IBM® SPSS® Statistics 25 software.

## 3. Results

### 3.1. Quantification of the Active Pharmaceutical Ingredient (API)

The calibration curve was prepared using known concentrations of acetaminophen as the active ingredient, and from this curve, the content in the biopolymeric film was determined, according to Lambert Beer's law. The analysis was performed by ultraviolet-visible spectrophotometry at 243 nm, preparing five calibration standards (0.8%, 0.6%, 0.4%, 0.2%, and 0.02%) from a 1% solution prepared with 99% pure acetaminophen. Figure S2 (Supporting information) shows the results of the absorbances at each of the known concentrations. The experimental value of the concentration in the film was determined from the equation of the straight line obtained by linear regression (Eq. 2). The

calibration curve obtained for quantification presented good linearity and a high correlation coefficient value ( $R^2 = 0.9983$ ), which guarantees the precision of the value obtained.

$$y = mx + b \quad (2)$$

$$x = (2.815 - 2.7624) / 0.1128 = 0.47$$

$$\text{API (\%)} = 0.47 * 25 = 11.75\%$$

The absorbance result of the film presented a value of 2.815, which generated a calculated experimental concentration of 0.47%, as shown in Figure S1. From the concentration found, it was multiplied by the dilution factor, which in this case was 25, to obtain the final concentration of 11.75% of API in the film. To calculate the theoretical concentration of the ODF with API, we started with the concentration of the polymer mixture before drying in the oven; this concentration was theoretically 0.5%. Since 23 mL was taken from this film-forming solution, then the amount of API is 0.11965 g. This concentration gave a recovery percentage of 98% when compared to the experimental concentration.

$$\text{API (g)} = (0.5 \text{ g API} / 100 \text{ g}) * 23.93 \text{ g} = 0.11965 \text{ g}$$

$$\text{API (\%)} = (0.11965 \text{ g de API} / 0.9994 \text{ g}) * 100 = 11.97\%$$

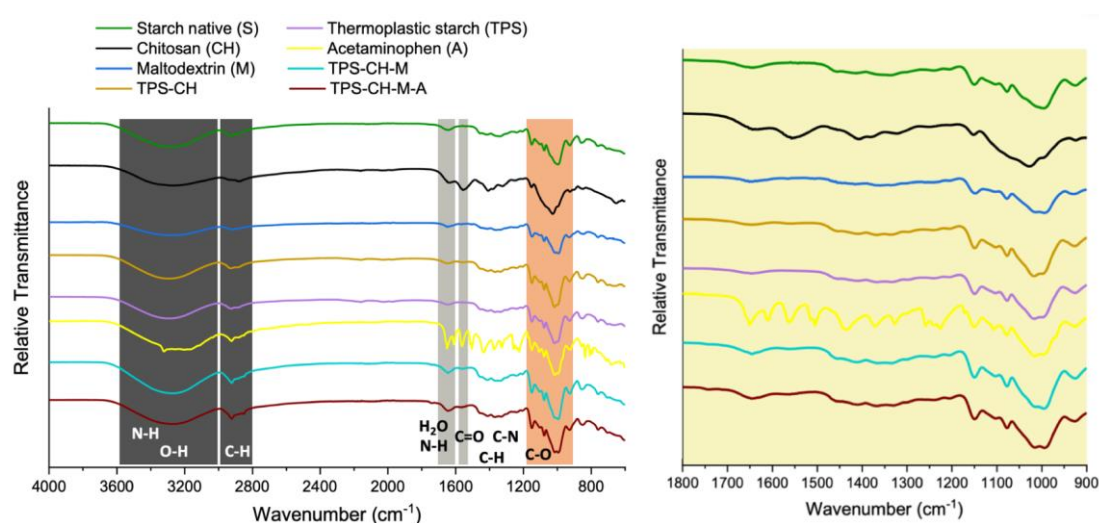
### 3.2. Fourier Transform Infrared (FTIR) Spectroscopy

Figure 1 shows the spectra obtained from the natural polymers of starch, chitosan, and maltodextrin, of which a broadband related to the stretching of the bonds is observed in the large region from  $3600 \text{ cm}^{-1}$  to  $3100 \text{ cm}^{-1}$ . O-H of the multiple hydroxyl groups of the participating molecules (glycerol, A) and macromolecules (biopolymers). In this same region, the vibration of the amino group (N-H) corresponding to chitosan (CH) and acetaminophen (A) appears located. Next, defined bands corresponding to asymmetric and symmetric stretching of C-H bonds were observed between  $2925 \text{ cm}^{-1}$  and  $2850 \text{ cm}^{-1}$ , respectively. These vibrations are related to the hydrocarbon chain, methyl, and methylene groups present in the different organic compounds. At a wavelength of  $\sim 1680 \text{ cm}^{-1}$ , the vibrational stretching mode of the carbonyl (C=O) present in the amides of chitosan is shown, which is partially deacetylated (up to 75%) and acetaminophen.[31] A nearby band appears at  $1695 \text{ cm}^{-1}$  of the water molecule, which achieved strong interactions with the other components until crystallization was achieved in the system. Another region of great importance in the spectrum corresponds to C-O interactions (ether zone) that begin at  $\sim 1300 \text{ cm}^{-1}$  up to  $949 \text{ cm}^{-1}$ . [32] In this area, significant changes are evident corresponding to hydrogen bond interactions between the different components as has been discussed and published in previous works. Finally, it was found that in the area known as fingerprints bands appear at  $838 \text{ cm}^{-1}$  and  $514 \text{ cm}^{-1}$  which are related to characteristic vibrations of the disubstituted aromatic ring in the para (p-) position and the deformation of the phenyl ring outside the plane, respectively. For the TPS-CH-M-A samples, some intensity changes can be seen in characteristic bands for API over the control (TPS-CH-M) as a result of the addition of =C-OH groups of the phenol (as part of the molecule of acetaminophen). Also, a change is observed in the ratio of bands  $1016 \text{ cm}^{-1}$  and  $990 \text{ cm}^{-1}$  that becomes similar to the API in the TPS-CH-M-A with respect to TPS-CH-M. This large region appears wider due to the limited intermolecular interactions that occur with the incorporation of the aromatic molecule, which causes steric hindrance in the mixture and low polarity. In general, no new bands are evident that could induce intramolecular reactions in the combination of components. For application purposes, it is very important to maintain the active component without structural changes.

Previously, the presence of functional groups in the structure of the polysaccharides used was discussed: starch, maltodextrin, and chitosan. The prominent -OH and -NH<sub>2</sub> groups provide hydrophilic properties; Furthermore, chitosan exhibits biosorbent qualities, including cationic and macromolecular structures with excellent sorption capacity.[33] According to studies carried out by Nawaz et al. 2023[34], different interaction mechanisms in which biopolymers participate are recognized, such as electrostatic attraction, electron donor-acceptor interactions ( $\pi$ - $\pi$ ), and hydrogen



bonds.[35] In this case, the acidic conditions are used to solubilize the chitosan and achieve optimal miscibility in the film-forming mixture (the previous solution reaches the solid state). In solution, the ability to interact between components is enhanced using mechanical and ultrasonic means during mixing. The slightly acidic pH (very close to neutrality) maintains the positive charge of the group ( $\text{NH}_2$ ) and achieves maximum adsorption, discussed by other authors through the calculation of thermodynamic properties, showing that it is spontaneous, endothermic, and based on a physisorption mechanism.[36] The interaction model proposed from the infrared analysis fits the one presented in Figure 2a where the individual components of each mixture are presented, including the TPS-CH-M plasticizers. In the case of the mixture that includes acetaminophen (TPS-CH-M-A, Figure 2b), an interaction model is presented that allows recognition of the integration in the system where Van der Waals interactions participate. Acetaminophen has a small size, which allows it to easily reach the interior and distribute evenly in the mixture. This will allow maximum interaction with the biopolymers, without transformation or modification in the structure through cross-linking reactions, and esterifications, among others.



**Figure 1.** FTIR spectra of the individual and mixed components involved in the biopolymeric films studied a) spectrum 4000  $\text{cm}^{-1}$  and 500  $\text{cm}^{-1}$ , and b) amplification 1800  $\text{cm}^{-1}$  and 900  $\text{cm}^{-1}$ .

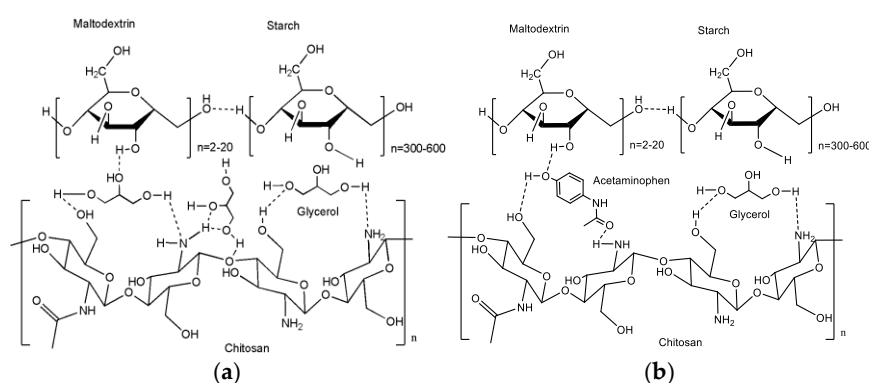


**Figure 2.** Molecular interaction models of a) TPS-CH-M and b) TPS-CH-M-A.

### 3.3. X-Ray Diffraction (XRD) Analysis

Figure 3 shows the diffraction patterns of the biopolymer films and the active ingredient, both as a mixture and independently. A large band ( $<10^\circ$  and  $\sim 30^\circ$ ) is observed in the TPS-CH-M blend, which reaches its maximum at  $13.8^\circ$  ( $2\theta$ ) as a product of the mixture between chitosan, maltodextrin, and starch, which has an amorphous structure according to this analysis. Concerning acetaminophen and, according to the X-ray pattern, a crystalline structure is observed, this result is as expected due to acetaminophen being a drug with polymorphs, the identified planes at  $15.6^\circ$ ,  $23.9^\circ$ ,  $26.4^\circ$  and  $32.5^\circ$

$2\theta$  correspond to planes (101), (211), (-220) and (-311), respectively.[37] According to the indexing of the X-ray pattern, the acetaminophen employed in this work has a monoclinic structure or Form I.[38] The TPS-CH-M-A film showed small peaks at  $23.5^\circ$  and  $32.3^\circ$   $2\theta$  that, according to the X-ray pattern of API, correspond to the API present in the edible film. The incorporation of API in the film TPS-CH-M promotes a light modification in the crystal structure of API due to the peaks showing a shift to minor angles from which it is inferred that there is an expansion in the unit cell of Form I, this result can be associated with high interaction of the API with the TPS-CH-M to such an extent that the unit cell of the API is affected to some extent.

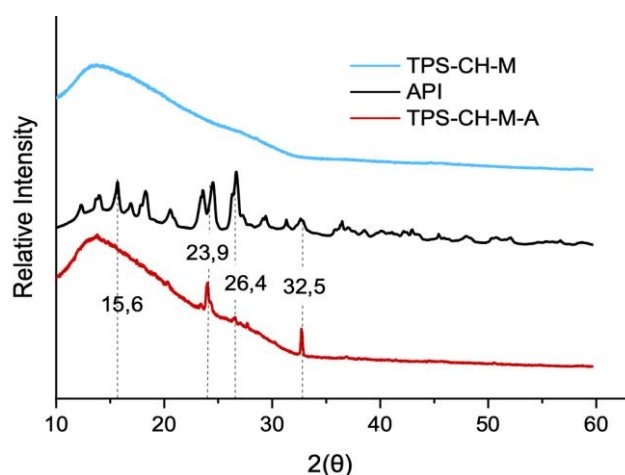


**Figure 3.** XRD patterns of TPS-CH-M and TPS-CH-M-A.

### 3.4. Simultaneous Thermal Analysis (TGA-DSC)

The thermal behavior of the films based on starch, chitosan, maltodextrin, and the active pharmaceutical ingredient was analyzed by TGA and DSC as evidenced in Figure 4 and 5, respectively. For the TGA curves and the respective derivatives (DTG) obtained for each polymer mentioned above, two very similar stages of mass loss are identified. The first stage is around  $100^\circ\text{C}$ , which is attributed to the loss of water and volatile matter, and the second stage is around  $300^\circ\text{C}$  which suggests the degradation and decomposition of the compound. When comparing the samples with each other, the thermal behaviour of the TPS shows the lowest thermal stability under a constant weight loss represented by the maximum slope in the range of  $25^\circ\text{C}$  up to  $270^\circ\text{C}$  in the comparison. Thus, the TGA thermogram of the TPS film demonstrated a weight loss in three stages. In the first stage, the loss of moisture was observed at a temperature below  $100^\circ\text{C}$ . The second stage indicated the degradation of the plasticizer between  $250$  and  $275^\circ\text{C}$ . The third stage is related to the decomposition of the polymeric material between  $300^\circ\text{C}$  and  $350^\circ\text{C}$ . The above is corroborated by the DSC curve, through the endothermic peaks. As for the active ingredient (acetaminophen), a moisture loss of  $\sim 15\%$  is observed in the TGA curve, followed by excellent stability in which the mass content is not altered. The initial degradation temperature ( $T_0$ ) is observed at  $272^\circ\text{C}$  and it ends at  $354^\circ\text{C}$  (final degradation temperature,  $T_f$ ). The thermal behavior in the ternary mixture TPS-CH-M allows us to infer from the result the presence of weak interactions due to intermolecular forces. This is because in polymers the high viscosity in physical mixtures and the steric hindrance at the structural level generated by the coiled polymer chains limit the possibility of interaction with other polymers.[39] The TPS-CH-M blend presented a maximum degradation temperature equal to  $290^\circ\text{C}$ , while the TPS-CH-M-A blend decreased its value significantly by  $20^\circ\text{C}$ . The incorporation of the pharmaceutically active ingredient in a solid state is distributed and inserted between the polymer chains limiting the interactions and blocking the dissipation of thermal energy.[40] DSC allows us to understand the thermal transitions inherent to different materials. Neat starch shows a second-order transition (see, broad band between  $50^\circ\text{C}$  to  $65^\circ\text{C}$ ). On the other hand, starch in the presence of plasticizers (TPS) and under thermomechanical process conditions presents an increase in heat

absorption due to the change in the polymeric network. This process is known as gelatinization and the properties are dependent on the plasticizer content. For TPS, a transition in the heat flow is observed that starts at  $\sim 50$  °C, reaching an endothermic minimum at 87.9 °C. It is observed that this process concludes at  $\sim 150$  °C. Similarly, to the above, maltodextrin presents a less pronounced endothermic event near 100 °C. The glass transition of chitosan is located at 67.4 °C located within an endothermic band that continues up to  $\sim 100$  °C related to the evaporation of solvents: water and acetic acid. The TPS-CH and TPS-CH-M mixtures showed complete gelatinization from the multiple intermolecular interactions between polymers. These mixtures show a gain in thermal stability corroborated in the TGA with the increase in degradation temperatures. Also, the transitions are delayed reaching a  $T_g$  equal to 124.7 °C and  $T_m$  equal to 156.8 °C. These results also proved not to be comparable with those obtained in the molten state and reactive extrusion, reiterating the importance and incidence of the variables of the mixing process.[4] The melting temperature of acetaminophen is 86.2 °C, with around 40 °C above and below, due to the polymorphism that this compound experiences.[42,43] The glass transition of TPS-CH-M-A is around 70 °C, located within an endothermic peak that continues up to 110 °C related to the volatilization of solvents and plasticizers. In the case of TPS-CH-M, the melting temperature and the glass transition peak are not detected. The above highlights the susceptibility to change experienced in the polymeric matrix due to interactions of the active ingredient [44].

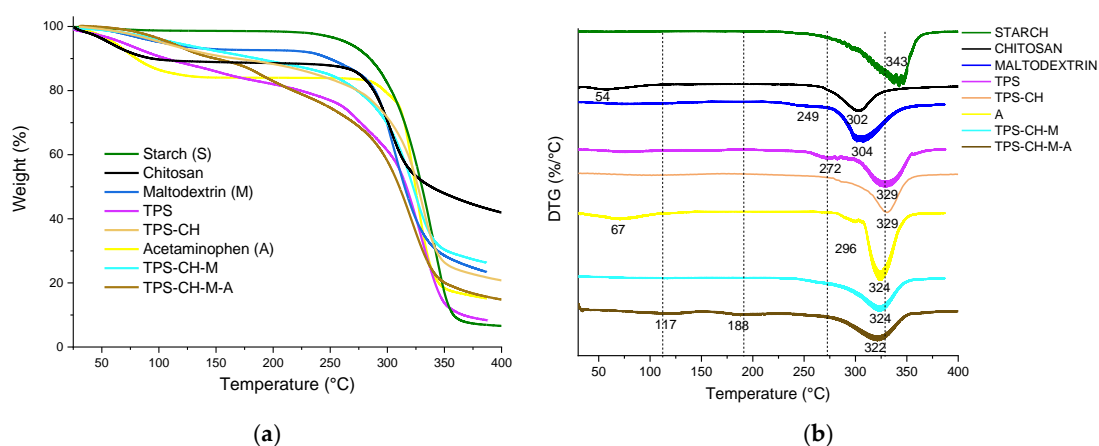


**Figure 4.** a) TGA and b) DTG curves of the different components used in the production of films with and without API.

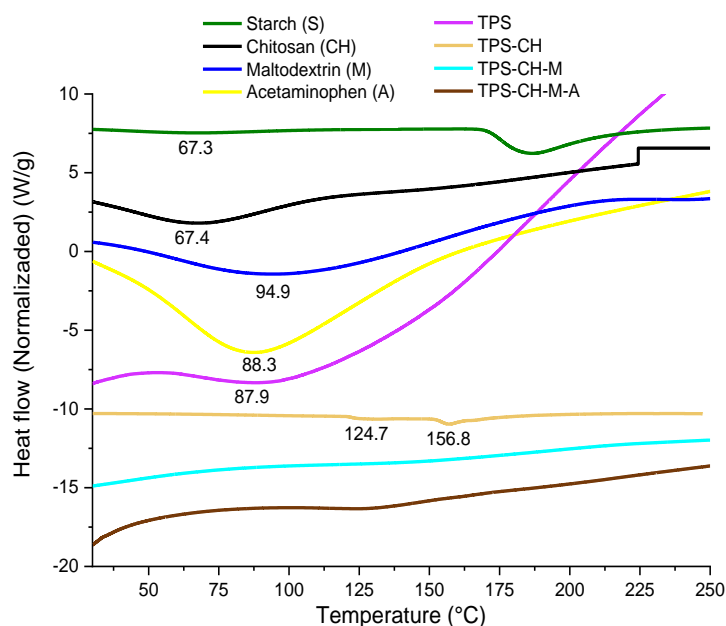


**Figure 5.** DSC curves of the different components used in the production of films with and without API.

3.5. Mechanical Tests

The mechanical performance of TPS-CH-M and TPS-CH-M-A are shown in Table 1, these values were calculated from the stress-strain graph of TPS-CH-M and TPS-CH-M-A films, a uniaxial tensile test until failure was used, in Figure 6 is shown the stress-strain curve of TPS-CH-M and TPS-CH-M-A films. According to the stress-strain of both curves, TPS-CH-M and TPS-CH-M-A films, it is possible to observe two areas, the elastic region, and the plastic region wherewith it is possible to define the mechanical behavior in both materials as plastic, a common behavior in biopolymer thermoplastics.[45] In the plastic region, the TPS-CH-M film shows an elastic area smaller than the TPS-CH-M film, and this change promotes a higher Elastic module in film with API increasing from 9.27 MPa for TPS-CH-M to 9.38 MPa for TPS-CH-M-A, this increase can be associated to the incorporation of API to film which is derivated for an elastomer behavior to the beginning of the elastic area in the film with API.[46] Also, the narrowing in the yield zone is observed to film with API promote a yield point lower for TPS-CH-M-A of 17.67 MPa while to TPS-CH-M is of 17.17 MPa. Also, the incorporation of API to the film TPS-CH-M causes the film’s break to a small non-uniform plastic deformation due to in the TPS-CH-M the Tensile strength Yield and the Breaking point have the same value of 24.21 MPa. In comparison, to TPS-CH-M-A the values are different at 24.54 MPa and 23.39 MPa for Tensile strength Yield and the Breaking point, respectively. In general, the incorporation of API into film promotes a higher tenacity in the film due to that the tenacity in the film with API increased 8%, hence, the incorporation of API into edible film is an improvement for the mechanical properties.

**Table 1.** The mechanical performance of TPS-CH-M and TPS-CH-M-A.

Mechanical properties	ODF Pristine	ODF with API
E (MPa)	9.27	9.38
Yield point (MPa)	17.76	17.67
Tensile strength Yield (MPa)	24.21	24.54
Breaking point (MPa)	24.21	23.39
Resilience (MPa)	17.84	15.04
Tenacity (MPa)	61.28	66.01

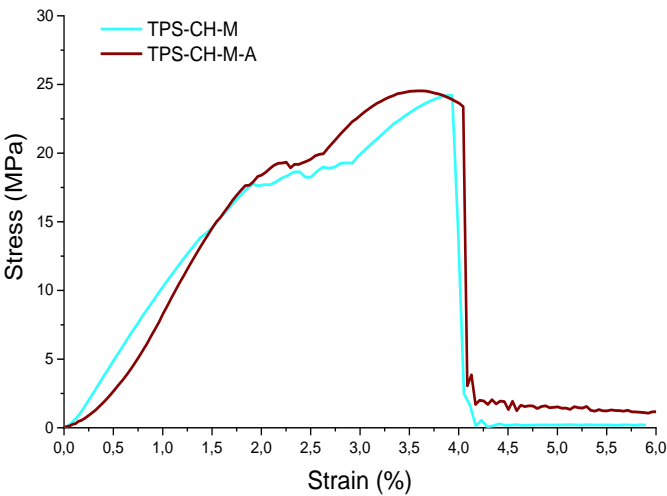


**Figure 6.** Tensile strength and elongation at break of the films with and without acetaminophen.



### 3.6. Scanning Electron Microscopy (SEM)

The profile morphology of TPS-CH-M and TPS-CH-M-A films was analyzed by SEM and it is presented in Figure 7. The profile of TPS-CH-M and TPS-CH-M-A shows a regular surface without cracks also the films are homogeny, the porosity is not possible to observe in both films, the incorporation of API to edible film is evident in the morphology due to is possible to observe a homogeny distribution of the cumulus which can be associated with the presence of API along the TPS-CH-M-A, while in TPS-CH-M is a homogeny and dense film.

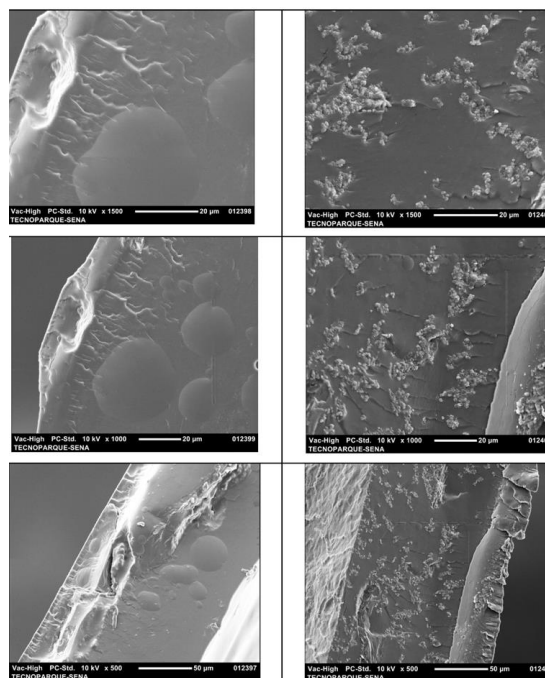
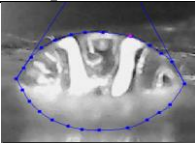
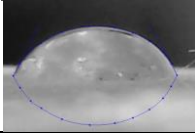


**Figure 7.** SEM micrographs of a) TPS-CH-M and b) TPS-CH-M-A films.

### 3.7. Contact Angle

The contact angle results presented in Table 2 for the TPS-CH-M and TPS-CH-M-A films remained without significant differences. According to the reported values, the nature of chitosan predominates, which has been reported in previous studies. It is important to mention that these values ( $69.18^\circ$ ) fall in the range of hydrophilic compounds responding to short analysis times (30 s).[47] However, the water absorption results change drastically between the two films, increasing the absorption of TPS-CH-M-A by 90% compared to the TPS-CH-M control. This could be because the acetaminophen particles, being uniformly distributed throughout the matrix, limit interactions between polymer chains, and allow a greater number of water molecules to enter and interact during the time they are submerged. This could be due to the fact that the acetaminophen particles, being uniformly distributed throughout the matrix, limit interactions between polymer chains, and allow a greater number of water molecules to enter and interact during the time they are submerged. The TPS-CH-M showed a contact angle of  $62.18^\circ \pm 0.12^\circ$ , which indicates it is a hydrophilic material due to its lower than  $90^\circ$ [48], and, the incorporation of API in edible film promotes a small increase in contact angle due to the value going to  $62.91^\circ \pm 0.03^\circ$ , however, the wettability in both films are hydrophilic. The results suggest that API does not have a considerable effect on the wettability of TPS-CH-M. Concerning the absorption of water (AW) in the TPS-CH-M-A is clear that the incorporation of API in the film promotes the absorption of water due to the TPS-CH-M showed AW of 321.28% while the TPS-CH-M-A showed AW of 410% the increase was of 28%, this result is convenient due to the film can have a more rapid disintegration because the water promotes this phenomenon.

**Table 2.** Contact angle and water absorption (AW) at the surface of films TPS-CH-M and TPS-CH-M-A.

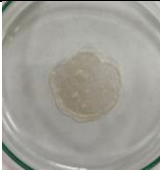











Sample	Contact angle (°) and picture		AW (%)
TPS-CH-M	62.18 ± 0.12		321.28 ± 2.85
TPS-CH-M-A	62.91 ± 0.03		410.52 ± 3.03

3.8. In Vitro Disintegration Test

3.8.1. In Vitro Oral Disintegrating Time

According to the results obtained in Table 3, the images show the formation of a gel related to starch and chitosan polymers.[49] There has been extensive discussion about applications of starch-based films as edible coatings, which can form gels when in contact with water. The polymer structure loses compaction (increases free volume) due to the exchange of kinetic energy of the water molecules at the time of interaction. This is because this system exceeds the energy of the hydrogen bonds present in the macromolecule. At this point, the starch gradually absorbs water until the granules complete their destructuring, burst, and form a new mixture of viscous consistency and flow.[50] Similarly, with chitosan, the hydroxyls of the water are introduced, decreasing the availability of hydroxyl groups, reducing intramolecular hydrogen bonds, and impacting solubility. In this sense, water is a strong donor and acceptor of hydrogen bonds, which makes it an excellent candidate for gelling chitosan. Thus, water molecules are incorporated into the chitosan network, and therefore destroy the three-dimensional structure of its molecules.[51] By breaking hydrogen bonds, molecular mobility increases, and as a result the films are more flexible.[52] The test performed on the disintegration time was determined by placing the film in a Petri dish containing a volume of water at 37 °C as has been studied by other authors.[53,54,55] To avoid subjectivity in the detection of the endpoint of the film, the release of the API from gradual measurements in solution was established as a criterion, in addition to the criterion of observing rupture or tendency of the film to swell in the sample holder. In this case, the fracture was observed, accompanied by a significant increase in diameter from minute 0 to 5, in addition to being translucent, a sign of the fluidity of the polymeric film.

**Table 3.** Picture of films in contact with water at 37 °C.

Sample	Time (min)					
	0	5	8	10	15	30
TPS-CH-M						
TPS-CH-M-A						

### 3.8.2. In Vitro Dissolution Time

Gradual measurements of the release profile of the API incorporated in the polymeric matrix were made from dissolution. This was evaluated by determining the concentration of the compound released over time. To simulate the salivary mucosa, the analysis was carried out in an aqueous medium at pH: 6.8. From the results obtained, it was possible to verify that the polymeric film took 10 min to release about 73% of the API and 15 min to release the entire active ingredient, to finally maintain its concentration constant after 30 min (See, Figure 8). Given these results, the proposed ODF can be classified as a very fast dissolving dosage form, since, according to the WHO, a drug is considered very fast dissolving when no less than 85% of the labeled amount of the drug has dissolved in 15 min, at pH 6.0 and 7.4 under the established conditions.[53] The fast release time obtained is directly attributed to the polymers used in the preparation of the ODF since the release rate can be influenced by hydrophilic or hydrophobic characteristics of all the components of the matrix, as well as the interaction between them can significantly influence the dissolution rate of the active ingredient. Generally, the use of a hydrophilic polymer such as chitosan or starch allows a rapid solution upon contact with saliva, releasing the active compound efficiently. On the other hand, the direct influence of thickness on disintegration times was corroborated, since initially these times ranged between 90 s to 120 s for films with thicknesses of 1.0 mm, while thicknesses of 0.04 mm decreased in time to 48 s.[56] Under this condition, the film presented a low disintegration time (< 60 s), according to the Ph.Eur.[57] The acceptance criterion for ODF disintegration time is “fast” and could vary between 30 s and 180 s.[57]

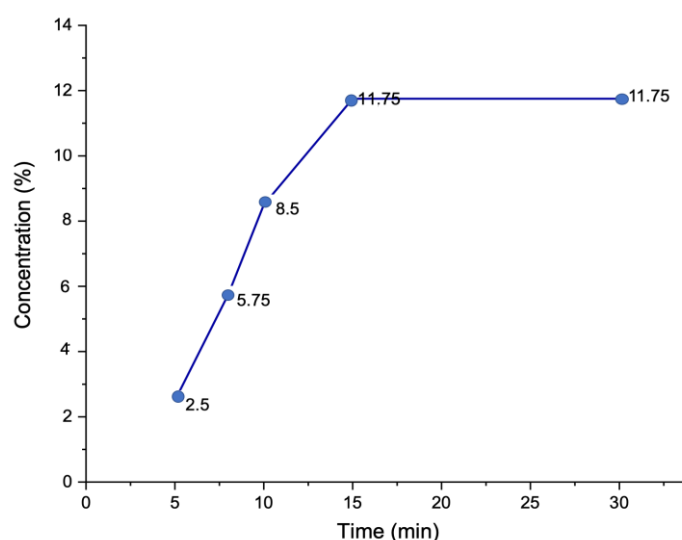


**Figure 8.** Drug concentration values released at certain dissolution times.

### 2.8.3. Total Soluble Solids (TSS)

The sugar content of the samples was determined under the same conditions as the in vitro dissolution tests. Figure 9 shows dissolved sugars (°Brix) results for the TPS-CH-M and TPS-CH-M-A samples. In general, an increase in values is observed as the dissolution time progresses.<sup>58</sup> This effect is more pronounced in the first 5 min for the TPS-CH-M-A sample compared to TPS-CH-M. The increase in values is indicative of the release of the oligosaccharide maltodextrin into the solution and partial disintegration of the starch.[59] This is caused by the free volume generated by the acetaminophen particles in the middle of the polymer chains. The particles open spaces that are easily occupied by water molecules in the dissolution process. This behavior is similar to that found in microencapsulation systems from a mixture of polysaccharides reported by Zahid-Hasan et al., 2023.[60] Likewise, the result of item 3.7 was corroborated, which explains how the sugars dissolved

in the products absorb moisture, limiting the aqueous medium. After 10 min, it is observed that the values are similar and at this point, they are already negligible for ODF applications.

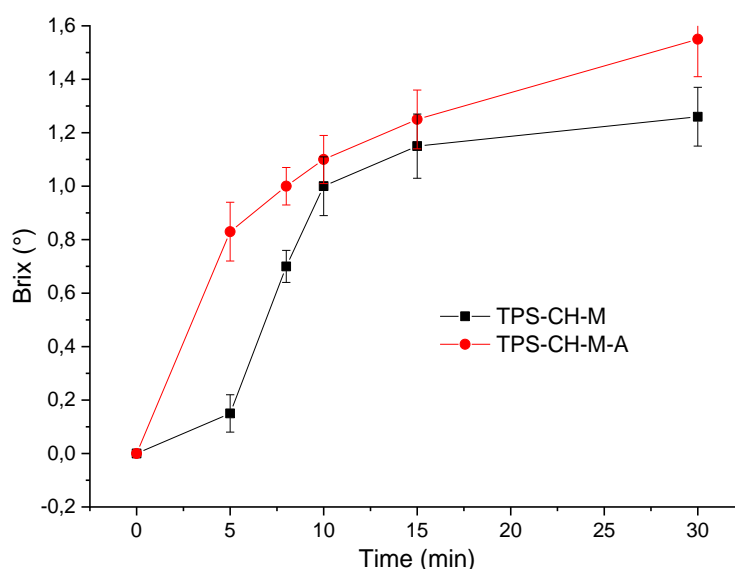


**Figure 9.** Picture of films in contact with water at 37 °C.

#### 4. Discussion

According to the physical-chemical results of the films TPS-CH-M and TPS-CH-M-A, the incorporation of API in a 0.5% p/p at filmogenic solution of TPS-CH-M allows to obtain a film with good properties for ODF applications, due to the density of this film is 1.554 g/mL, and, the quantification of the API in the film demonstrated that the model drug employed is loaded close to 11.75% in the total mass of the polymer film. Hence, a typical size of the ODF is 3 cm x 2 cm so in a TPS-CH-M film total mass is 37.2 mg and the total load of the model drug is close to 4.37 mg. Therefore, this film can be a proposal to be employed in other kinds of drugs where the dose is closer to 4 mg and also can be solubilized in water such as naloxone a drug that rapidly reverses an opioid overdose and the dose is close to 0.4 mg, or other drugs that can be solubilized in ethanol or a mix of ethanol/water such as loperamide a drug used in acute diarrhea.

#### 5. Conclusions

The preparation of an edible film based on starch-chitosan-maltodextrin capable of supporting a drug model as acetaminophen was possible opening the possibility to use this film in loading other drugs which doses in low. This film can be employed as a ODF. The physicochemical properties of ODF demonstrated that the preparation method was optimal by allowing miscibility between the polymeric components, besides reaching a homogeneous distribution of the acetaminophen particles along the ODF, which was corroborated by morphological analysis. The dispersion of the drug can be improved by physical methods so that drug model, the acetaminophen particles do not accumulate. The infrared spectroscopy technique demonstrated the intermolecular interactions between the polymeric chains and the active ingredient. Likewise, X-ray diffraction analysis showed an expansion in the monoclinic cell that projects the ordering of the drug. The ordering of atoms to long range in the polymer blend is non-existent, hence, the structure is amorphous, also, the drug does not promote chemical reactions. Thermal analysis by DSC confirmed the state changes for the mixtures that experienced first-order transitions such as melting, where the drug's fusion enthalpy decreases, and second-order transitions such as gelatinization (disappearance) of the polymeric components in the mixture. In contrast, the degradation temperatures had a similar behavior in TPS-



CH-M and TPS-CH-M-A. The mechanical properties such as maximum strength, toughness, and elastic modulus were slightly favored suggesting a mechanical behavior in TPS-CH-M-A close to composite material. Regarding the hydrophilic properties of the film detected in the contact angle test and subsequent water absorption analysis, a 28% increase was achieved in the film with API compared to the TPS-CH-M control. Water allows the degradation of polysaccharides, favoring the increase of soluble solids and the release of the drug.

**Supplementary Materials:** The following supporting information can be downloaded at the website of this paper posted on Preprints.org, Figure S1 and Figure S2.

**Author Contributions:** Conceptualization, C.C. and A.F.G.; methodology, C.C.; software, C.C.; validation, C.C. and A.F.G.; formal analysis, C.C., A.F.G., N.R.G., L.P. and L.S.; investigation, C.C., A.F.G., N.R.G., L.P. and L.S.; resources, C.C. and A.F.G.; data curation, C.C. and A.F.G.; writing—original draft preparation, C.C., A.F.G., N.R.G., L.P. and L.S.; writing—review and editing, C.C. and H.L.C.P.; visualization, C.C.; supervision, C.C. and A.F.G.; project administration, C.C.; funding acquisition, C.C. All authors have read and agreed to the published version of the manuscript.

**Funding:** This research received no external funding.

**Institutional Review Board Statement:** Not applicable.

**Informed Consent Statement:** Not applicable.

**Data Availability Statement:** Data are contained within the article.

**Acknowledgments:** This research was funded by Vice-Rector for Research of Unidad Central del Valle del Cauca under project No. PI-1300-50.2-2024-PDP11. The authors thanks to Ing. Beatriz E. Reyes Vielma for the technical support.

**Conflicts of Interest:** The authors declare no conflicts of interest.

## References

1. Pacheco, M.S.; Barbieri, D.; da Silva, C.F.; de Morales, M.A. A review on orally disintegrating films (ODFs) made from natural polymers such as pullulan, maltodextrin, starch, and others. *Int. J. Biol. Macromol.* **2021**, *178*, 504–513. [CrossRef]
2. Ariza-Galindo, C.J.; Rojas Aguilar, D.M. Disfagia en el adulto mayor. *Univ. Med.* **2020**, *61*, 117–128. [CrossRef]
3. Turković, E.; Vasiljević, I.; Drašković, M.; Parojčić, J. Orodispersible films—Pharmaceutical development for improved performance: A review. *J. Drug Deliv. Sci. Technol.* **2022**, 103708. [CrossRef]
4. dos Santos Garcia, V.A.; Borges, J.G.; Vanin, F.M.; de Carvalho, R.A. Orally disintegrating films of biopolymers for drug delivery. *Biopolymer Membranes and Films* **2020**, 289–307. [CrossRef]
5. Zhou, Y.; Wang, M.; Yan, C.; Liu, H.; Yu, D.G. Advances in the Application of Electrospun Drug-Loaded Nanofibers in the Treatment of Oral Ulcers. *Biomolecules* **2022**, *12*, 1254. [CrossRef]
6. Alopaeus, J.F.; Hellfritzsche, M.; Gutowski, T.; Scherließ, R.; Almeida, A.; Sarmiento, B.; Tho, I. Mucoadhesive buccal films based on a graft co-polymer—A mucin-retentive hydrogel scaffold. *Eur. J. Pharm. Sci.* **2020**, *142*, 105142. [CrossRef]
7. He, M.; Zhu, L.; Yang, N.; Li, H.; Yang, Q. Recent advances of oral film as platform for drug delivery. *Int. J. Pharm.* **2021**, *604*, 120759. [CrossRef]
8. Xu, Y.X.; Kim, K.M.; Hanna, M.A.; Nag, D. Chitosan–starch composite film: preparation and characterization. *Ind. Crops Prod.* **2005**, *21*, 185–192. [CrossRef]
9. Haugstad, K.E.; Håti, A.G.; Nordgård, C.T.; Adl, P.S.; Maurstad, G.; Sletmoen, M.; Stokke, B.T. Direct determination of chitosan–mucin interactions using a single-molecule strategy: Comparison to alginate–mucin interactions. *Polymers* **2015**, *7*, 161–185. [CrossRef]

10. do Vale, D.A.; Vieira, C.B.; Vidal, M.F.; Claudino, R.L.; Andrade, F.K.; Sousa, J.R.; de Souza, B.W.S. Chitosan-Based Edible Films Produced from Crab-Uçá (*Ucides cordatus*) Waste: Physicochemical, Mechanical and Antimicrobial Properties *J. Polym. Environ.* 2021, 29, 694–706. [CrossRef]
11. Jimenez, A.; Fabra, M.J.; Talens, P.; Chiralt, A. Edible and Biodegradable Starch Films: A Review. *Food Bioprocess Technol.* 2012, 5, 2058–2076. [CrossRef]
12. Kim, K.W.; Lee, B.H.; Kim, H.J.; Sriroth, K.; Dorgan, J.R. Thermal and mechanical properties of cassava and pineapple flours-filled PLA bio-composites. *J. Therm. Anal. Calorim.* 2012, 108, 1131–1139. [CrossRef]
13. Olomo, V.; Ajibola, O. Processing factors affecting the yield and physicochemical properties of starch from cassava chips and flour. *Starch-Stärke* 2003, 55, 476–481. [CrossRef]
14. Abera, B.; Duraisamy, R.; Birhanu, T. Study on the preparation and use of edible coating of fish scale chitosan and glycerol blended banana pseudostem starch for the preservation of apples, mangoes, and strawberries. *J. Agric. Food Res.* 2024, 15, 100916. [CrossRef]
15. Barranco-García, J.E.; Caicedo, C.; Jiménez-Regalado, E.J.; Espinoza-González, C.; Morales, G.; Aguirre-Loredo, R.Y.; Fonseca-García, A. The potential of starch-chitosan blends with poloxamer for the preparation of microparticles by spray-drying. *Particuology* 2024, 89, 1–10. [CrossRef]
16. Amalia, A.; Nining, N.; Dandi, M. Characterization of modified sorghum starch and its use as a film-forming polymer in orally dissolving film formulations with glycerol as a plasticizer. *J. Res. Pharm.* 2023, 27, 1855–1865. [CrossRef]
17. Cupone, I.E.; Roselli, G.; Marra, F.; Riva, M.; Angeletti, S.; Dugo, L.; Giori, A.M. Orodispersible film based on maltodextrin: A convenient and suitable method for iron supplementation. *Pharmaceutics* 2023, 15, 1575. [CrossRef]
18. Chranioti, C.; Tzia, C. Thermooxidative Stability of Fennel Oleoresin Microencapsulated in Blended Biopolymer Agents. *J. Food Sci.* 2014, 79, C1091–C1099. [CrossRef]
19. Chranioti, C.; Nikoloudaki, A.; Tzia, C. Saffron and beetroot extracts encapsulated in maltodextrin, gum Arabic, modified starch and chitosan: Incorporation in a chewing gum system. *Carbohydr. Polym.* 2015, 127, 252–263. [CrossRef]
20. Brune, K.; Renner, B.; Tiegs, G. Acetaminophen/paracetamol: A history of errors, failures and false decisions. *Eur. J. Pain* 2015, 19, 953–965. [CrossRef]
21. Acheampong, P.; Thomas, S.H. Determinants of hepatotoxicity after repeated supratherapeutic paracetamol ingestion: Systematic review of reported cases. *Br. J. Clin. Pharmacol.* 2016, 82, 923–931. [CrossRef]
22. Huang, S.; Salim, M.; Barber, B.W.; Pham, A.C.; McDowell, A.; Boyd, B.J. Dissolution of pain-relief drugs: Does beverage choice matter? *J. Drug Deliv. Sci. Technol.* 2024, 91, 105247. [CrossRef]
23. Skoog, D.A.; Holler, F.J.; Nieman, T.A. *Principios de análisis instrumental*, 5th ed.; McGraw-Hill: Madrid, 2001; pp. 614–633.
24. Chan, S.Y.; Goh, C.F.; Lau, J.Y.; Tiew, Y.C.; Balakrishnan, T. Rice starch thin films as a potential buccal delivery system: Effect of plasticiser and drug loading on drug release profile. *Int. J. Pharm.* 2019, 562, 203–211. [CrossRef]
25. ASTM D882-12, Standard Test Method for Tensile Properties of Thin Plastic Sheeting; ASTM International.
26. Kumar, S.; Madan, S.; Bariha, N.; Suresh, S. Swelling and shrinking behavior of modified starch biopolymer with iron oxide. *Starch-Stärke* 2021, 73, 2000108. [CrossRef]
27. Butler, M.F.; Clark, A.H.; Adams, S. Swelling and Mechanical Properties of Biopolymer Hydrogels Containing Chitosan and Bovine Serum Albumin. *Biomacromolecules* 2006, 7, 2961–2970. [CrossRef]
28. Garsuch, V.; Breitreutz, J. Comparative investigations on different polymers for the preparation of fast-dissolving oral films. *J. Pharm. Pharmacol.* 2010, 62, 539–545. [CrossRef]
29. Okamoto, H.; Taguchi, H.; Iida, K.; Danjo, K. Development of polymer film dosage forms of lidocaine for buccal administration: I. Penetration rate and release rate. *J. Controlled Release* 2001, 77, 253–260. [CrossRef]
30. Helrich, K. *Official Methods of Analysis of the Association of Official Analytical Chemists*; Association of Official Analytical Chemists: 1990.

31. Trivedi, M.; Patil, S.; Shettigar, H.; Bairwa, K.; Jana, S. Effect of biofield treatment on spectral properties of paracetamol and piroxicam. *Chem. Sci. J.* 2015, 3, 6. [CrossRef]
32. Sritham, E.; Gunasekaran, S. FTIR spectroscopic evaluation of sucrose-maltodextrin-sodium citrate bioglass. *Food Hydrocolloids* 2017, 70, 371–382. [CrossRef]
33. Vakili, M.; Rafatullah, M.; Salamatnia, B.; Abdullah, A.Z.; Ibrahim, M.H.; Tan, K.B.; Amouzgar, P. Application of chitosan and its derivatives as adsorbents for dye removal from water and wastewater: A review. *Carbohydr. Polym.* 2014, 113, 115–130. [CrossRef]
34. Nawaz, S.; Tabassum, A.; Muslim, S.; Nasreen, T.; Baradoke, A.; Kim, T.H.; Bilal, M. Effective assessment of biopolymer-based multifunctional sorbents for the remediation of environmentally hazardous contaminants from aqueous solutions. *Chemosphere* 2023, 329, 138552. [CrossRef]
35. Fonseca-García, A.; Osorio, B.H.; Aguirre-Loredo, R.Y.; Calambas, H.L.; Caicedo, C. Miscibility study of thermoplastic starch/polylactic acid blends: Thermal and superficial properties. *Carbohydr. Polym.* 2022, 293, 119744. [CrossRef]
36. Gao, B.; Li, P.; Yang, R.; Li, A.; Yang, H. Investigation of multiple adsorption mechanisms for efficient removal of ofloxacin from water using lignin-based adsorbents. *Sci. Rep.* 2019, 9, 637. [CrossRef]
37. Jendrzewska, I.; Goryczka, T.; Pietrasik, E.; Klimontko, J.; Jampilek, J. X-ray and Thermal Analysis of Selected Drugs Containing Acetaminophen. *Molecules* 2020, 25(24), 5909. [CrossRef]
38. Perrin, M.A.; Neumann, M.A.; Elmaleh, H.; Zaske, L. Crystal structure determination of the elusive paracetamol Form III. *Chem. Commun.* 2009, 22, 3181. [CrossRef]
39. Walsh, D.J.; Rostami, S. The miscibility of high polymers: The role of specific interactions. In *Key Polymers Properties and Performance*; Springer Berlin Heidelberg: Berlin, Heidelberg, 2005; pp. 119–169. [CrossRef]
40. Cao, B.Y.; Kong, J.; Xu, Y.; Yung, K.L.; Cai, A. Polymer nanowire arrays with high thermal conductivity and superhydrophobicity fabricated by a nano-molding technique. *Heat Transfer Eng.* 2013, 34, 131–139. [CrossRef]
41. Merino, D.; Gutiérrez, T.J.; Alvarez, V.A. Potential Agricultural Mulch Films Based on Native and Phosphorylated Corn Starch With and Without Surface Functionalization with Chitosan. *J. Polym. Environ.* 2019, 27, 97–105. [CrossRef]
42. Sacchetti, M. Thermodynamic Analysis of DSC Data for Acetaminophen Polymorphs. *J. Therm. Anal. Calorim.* 2000, 63, 345–350. [CrossRef]
43. Bashpa, P.; Bijudas, K.; Tom, A.M.; Archana, P.K.; Murshida, K.P.; Banu, K.N.; Vimisha, K. A paracetamol-poly (3,4-ethylenedioxythiophene) composite film for drug release studies. *Int. J. Chem. Stud.* 2014, 1, 25–29. [CrossRef]
44. Awasthi, S.; Singhal, R. A study on interaction and solubility of acetaminophen with poly (AM-co-HEA-co-AA) hydrogels by DSC: Effect on drug diffusion behavior. *J. Macromol. Sci., Part A* 2013, 50, 72–89. [CrossRef]
45. Mendes, J.F.; Paschoalin, R.T.; Carmona, V.B.; Neto, A.R.S.; Marques, A.C.P.; Marconcini, J.M.; Oliveira, J.E. Biodegradable polymer blends based on corn starch and thermoplastic chitosan processed by extrusion. *Carbohydr. Polym.* 2016, 137, 452. [CrossRef]
46. Kim, T.K.; Kim, J.K.; Jeong, O.C. Measurement of nonlinear mechanical properties of PDMS elastomer. *Microelectron. Eng.* 2011, 88(8), 1982. [CrossRef]
47. Aguirre-Loredo, R.Y.; Fonseca-García, A.; Calambas, H.L.; Salazar-Arango, A.; Caicedo, C. Improvements of thermal and mechanical properties of achira starch/chitosan/clay nanocomposite films. *Heliyon* 2023, 9, 6. [CrossRef]
48. Ma, Y.; Cao, X.; Feng, X.; Ma, Y.; Zou, H. Fabrication of super-hydrophobic film from PMMA with intrinsic water contact angle below 90. *Polymer* 2007, 48(26), 7455–7460. [CrossRef]
49. Panraksa, P.; Tipduangta, P.; Jantanasakulwong, K.; Jantrawut, P. Formulation of orally disintegrating films as an amorphous solid solution of a poorly water-soluble drug. *Membranes* 2020, 10, 376. [CrossRef]
50. Wang, B.; Yu, B.; Yuan, C.; Guo, L.; Liu, P.; Gao, W.; Li, D.; Cui, B.; Abd El-Aty, A.M. An overview on plasticized biodegradable corn starch-based films: The physicochemical properties and gelatinization process. *Crit. Rev. Food Sci. Nutr.* 2022, 62, 2569–2579. [CrossRef]

51. Wang, S.; Jing, Y. Study on the barrier properties of glycerol to chitosan coating layer. *Mater. Lett.* 2017, 209, 345–348. [CrossRef]
52. Chen, M.; Runge, T.; Wang, L.; Li, R.; Feng, J.; Shu, X.L.; Shi, Q.S. Hydrogen bonding impact on chitosan plasticization. *Carbohydr. Polym.* 2018, 200, 115–121. [CrossRef]
53. Garsuch, V.; Breitzkreutz, J. Novel analytical methods for the characterization of oral wafers. *Eur. J. Pharm. Biopharm.* 2009, 73, 195–201. [CrossRef]
54. Garsuch, V.; Breitzkreutz, J. Comparative investigations on different polymers for the preparation of fast-dissolving oral films. *J. Pharm. Pharmacol.* 2010, 62, 539–545. [CrossRef]
55. El-Setouhy, D.A.; El-Malak, N.S.A. Formulation of a novel tianeptine sodium orodispersible film. *AAPS PharmSciTech* 2010, 11, 1018–1025. [CrossRef]
56. Pechová, V.; Gajdziok, J.; Muselík, J.; Vetchý, D. Development of orodispersible films containing benzydamine hydrochloride using a modified solvent casting method. *AAPS PharmSciTech* 2018, 19, 2509–2518. [CrossRef]
57. European Pharmacopoeia Commission. *European Pharmacopoeia*, 7th ed.; European Directorate for the Quality of Medicines (EDQM): Strasbourg, France, 2012; pp. 4257–4259.
58. Onkov, K.Z.; Kassamakov, I.V. Computer models for adjustment of fiber-optic refractometers for concentration measurement of sugar solutions. *Comput. Ind.* 1993, 21, 279–283. [CrossRef]
59. Xiong, Y.; Tian, C.; Zhu, J.; Zhang, S.; Wang, X.; Chen, W.; Han, Y.; Du, Y.; Wu, Z.; Zhang, K. Dynamic changes of starch properties, sweetness, and  $\beta$ -amylases during the development of sweet potato storage roots. *Food Biosci.* 2024, 104964. [CrossRef]
60. Hasan, M.Z.; Nupur, A.H.; Habiba, U.; Robin, M.A.; Akash, S.I.; Rawdkuen, S.; Mazumder, M.A.R. Incorporation of orange peel polyphenols in buttermilk, maltodextrin and gum acacia suspension improve its stability. *Food Hum.* 2023, 1, 1345–1354. [CrossRef]

**Disclaimer/Publisher's Note:** The statements, opinions and data contained in all publications are solely those of the individual author(s) and contributor(s) and not of MDPI and/or the editor(s). MDPI and/or the editor(s) disclaim responsibility for any injury to people or property resulting from any ideas, methods, instructions or products referred to in the content.